Available online at www.sciencedirect.com

ScienceDirect

Solar Energy 132 (2016) 511–517

SOLAR ENERGY

www.elsevier.com/locate/solener

Fe doped TiO_2 thin film as electron selective layer for inverted solar cells

Arif Kösemen [a,b], Zühal Alpaslan Kösemen [a,c], Betül Canimkubey [a,d], Mustafa Erkovan [e], Fevzihan Başarir [f], Sait Eren San [a,f], Osman Örnek [g], Ali Veysel Tunç [h,*]

[a] Department of Physics, Gebze Technical University, Kocaeli, Turkey
[b] Department of Physics, Muş Alparslan University, Muş, Turkey
[c] TUBİTAK UME Optics Laboratory, 41470 Gebze, Kocaeli, Turkey
[d] Deparment of Physics, Amasya University, Amasya, Turkey
[e] Materials Science and Engineering Department, Sakarya University, 54687 Sakarya, Turkey
[f] Materials Institute, TUBITAK MRC, 41470 Gebze, Kocaeli, Turkey
[g] Department of Metallurgy and Materials Engineering, Ahievran University, Kırşehir, Turkey
[h] Department of Energy Systems Engineering, Istanbul Bilgi University, 34060 Eyup, Istanbul, Turkey

Received 2 July 2015; received in revised form 7 October 2015; accepted 25 March 2016
Available online 7 April 2016

Communicated by: Associate Editor Sam-Shajing Sun

Abstract

Inverted P3HT:PCBM based organic solar cells were fabricated by using Fe^{2+} doped TiO_2 films as electron selective layer. Pure and Fe^{2+} doped TiO_2 films were prepared by sol–gel method and the optical as well as the structural properties of the thin films were characterized by UV–Vis spectrophotometer and SEM. The concentration of Fe^{2+} was varied as 0.5%, 1%, 2% and 3% (w/w) in TiO_2 layer and the influence of Fe^{2+} doping on the solar cell parameters were systemically investigated. Photocurrent density of the solar cells as increased from 8.75 to 13.8 mA/cm^2, whereas the solar cell efficiency changed from 1.7% to 2.79% by using Fe^{2+} doped TiO_2 electron selective layer. It was experimentally found and demonstrated that charge injection and selection in the TiO_2 interlayer was improved by doping of Fe^{2+} atoms in the TiO_2.

Keywords: Inverted type solar cells; TiO_2 thin film; Fe doped TiO_2 thin film; Doped metal oxide semiconductors

1. Introduction

There has been increasing demand for cost effective photovoltaic devices due to the global energy challenge. The market is dominated by silicon based photovoltaic devices; however, their wide utilization is limited by their high cost. Bulk-heterojunction (BHJ) type organic photovoltaic (OPV) seems the best alternative regarding cost efficiency. Therefore, recent years have witnessed the great research effort on organic solar cells (OPVs) owing to their low-cost as well as their mechanical flexibility, light weight, and possibility of large area fabrication (Andersen et al., 2014; Winkler et al., 2011). However, some of the disadvantages of OPVs are lowerpower conversion efficiency and shorter life times compared to their inorganic counterparts. Thus, most of the research activities have been performed on improving the power conversion efficiency of organic solar cells as well as satisfying long term stability of OPV devices during the last decade.

* Corresponding author.
E-mail address: aliveyseltunc@gmail.com (A.V. Tunç).

http://dx.doi.org/10.1016/j.solener.2016.03.049
0038-092X/

For instance, the efficiency of OPVs has been improved by synthesis of new donor and acceptor materials and manufacturing of new device structures (Yu et al., 1995; Liang et al., 2010). Conventional OPVs are typically constructed by sandwiching of active layer between the hole transport layer (PEDOT:PSS) and metal cathode, which has a low work function. BHJ type OPV includes p-type (donor) material and n-type (acceptor) material which are mixed in solvent and coated as active layer either on the positive or on the negative electrode. The blended electron donor and acceptor materials form 3-D thin film matrix. Incident light is absorbed by the active layer to create abounded electron–hole pairs (exciton), which can move together up to 10–20 nm (Su et al., 2012; Peumans et al., 2003). Exciton usually separates into charge carrier as electron and hole at the interface of the donor–acceptor materials. Hole moves toward to PEDOT:PSS coated ITO (anode) side and electron moves toward to metal contact (cathode). The life time of the organic solar cells is mostly determined by the contact materials. Recent studies showed that low work function metal cathode is easily affected by the ambient conditions. On the other hand, ITO was found to be quite sensitive to the acidic nature of PEDOT:PSS, which leads to corrosion on ITO surface (de Jong et al., 2000; Kawano et al., 2006; Girtan and Rusu, 2010; Norrman et al., 2006). To overcome the mentioned obstacles, inverted type OPVs have been proposed, which improved the stability of the devices (Li et al., 2006; Kuwabara et al., 2008; Norrman et al., 2010). In inverted type solar cells, the surface of the ITO electrode is modified with metal oxide materials such as ZnO, TiO_2 and Cs_2CO_3 so that ITO acts as a negative electrode (Hames et al., 2010; Yu et al., 2008; Liao et al., 2008). On the other hand, high work function metal layer such as Ag and Au etc. is coated on the active layer to collect the holes.

TiO_2 is a very commonly used material as an electron selective layer for inverted type solar cells because of its high optical transparency in the visible and near infra-red region as well as its high charge carrier mobility (Cheng et al., 2011; Lin et al., 2011; Wong et al., 2014). Recent research results demonstrated that the structural properties, photo reactivities, charge carrier recombination rates, interfacial electron transfer rates and magnetic properties can be easily manipulated, when TiO_2 is doped with some metal ions (Kim et al., 2014; Yuan et al., 2013; Alparslan et al., 2011). Nowadays, metal ion doped TiO_2 thin films as an electron selective layer are frequently used to improve solar cell efficiency (Xu et al., 2013; Thambidurai et al., 2014; Liu et al., 2014).

In this study, therefore, Fe doped TiO_2 inter layer were used to produce an inverted solar cell and the assembly has been constructed as ITO/Fe:TiO_2/P3HT:PCBM/V_2O_5/Ag. Pure and Fe^{2+} doped TiO_2 thin films were fabricated by sol–gel method. The optical and structural properties of the thin films were characterized by using SEM and UV–Vis spectrophotometer. Influence of Fe^{2+} doping in the TiO_2 interlayer on the efficiency of P3HT:PCBM based solar cell was studied. Fe^{2+} was introduced to TiO_2 via solution at concentrations ranging from 0 to 3 wt.% with respect to the weight of the TiO_2. Photocurrent density of the solar cells were increased from 8.75 to 13.8 mA/cm^2 and solar cell efficiencies from 1.7% to 2.79% by using Fe^{2+} doped TiO_2 as electron selective layer. This phenomenon indicates that actually charge injection and selection in the TiO_2 interlayer is effected by doping. The improvement in performance in terms of affect of charge injection and selection are correlated to the increase in solar cell efficiency and this was realized and discussed.

2. Experimental

P3HT (Aldrich) and PCBM (Aldrich) were used in the structure of active layer without any further purification. Their chemical formulas are given in Fig. 1(a) and (b), respectively. P3HT and PCBM were firstly mixed in 1,2 dichlorobenzene with 1:1 (wt/wt) ratio and stirred at 50 °C overnight. In order to prepare TiO_2 sol–gel mixture; titanium n-butoxide, ethanol, isopropanol alcohol, and acetic acid were mixed with (1:20:20:0.15) molar ratio, respectively, for 48 h at room temperature. Also, $FeCl_2$ was added into a solution containing a mixture of ethanol, isopropanol alcohol, and acetic acid molar ratio of 1:20:20:0.15. This solution was stirred for two hours at room temperature, and then titanium n-butoxide was added to this sol–gel mixture to prepare Fe-doped TiO_2 sample. Ti amount in the solution is proportional to the amount of Fe, at ratio of their weights. The Fe amounts in samples were prepared as 0.5%, 1%, 2% and 3%. In regard to the solar cell fabrication process, ITO coated glass was firstly subject to a standard cleaning process with acetone, ethanol, and distilled water in ultrasonic bath for 15 min. TiO_2 and Fe doped TiO_2 solutions were coated with spin coater at 3500 rpm 25 s., followed by annealing at 400 °C for 30 min with a heating rate of 10 °C/min. The solar cells were designed with ITO/TiO_2/P3HT:PCBM/V_2O_5/Ag and ITO/Fe:TiO_2/P3HT:PCBM/V_2O_5/Ag configuration as shown in Fig. 1(c) and (d). Next, P3HT:PCBM was coated at 800 rpm as active layer on the TiO_2 films. Then, V_2O_5 (10 nm) and Ag (100 nm) was deposited as hole transport and contact layers, respectively. Current–voltage characteristics of the samples were analyzed with (Keithley 4200 SCS) semiconductor characterization system and (Thermo Oriel) Solar Simulator under AM1.5G (100 mW/cm^2) with standard characterization regulations. Solar simulator was calibrated with reference photodiode.

3. Results and discussion

Morphological properties of the Fe doped and pure TiO_2 thin films were investigated via scanning electron microscopy (SEM). Fig. 2 shows the SEM images of the produced Fe doped and pure TiO_2 thin films by spin casting from solution. It is clearly seen from Fig. 2 that

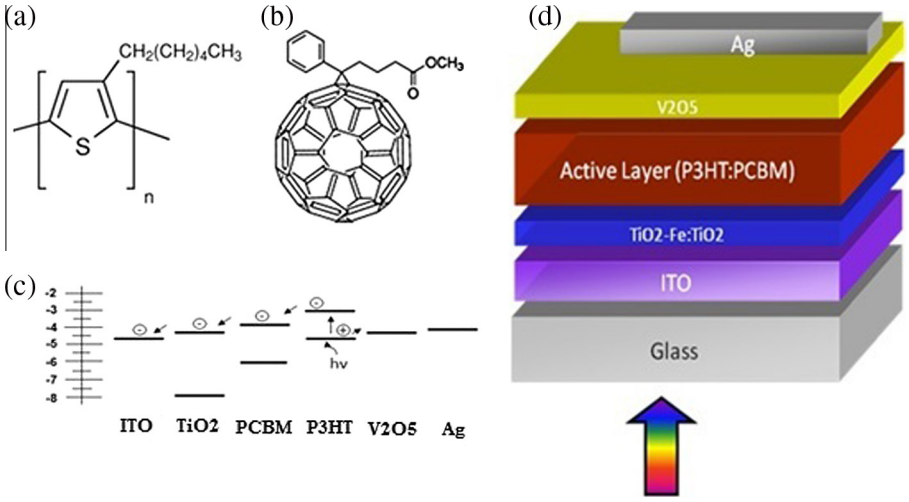

Fig. 1. (a) Molecular structure of the P3HT and (b) PCBM, (c) energy diagram of the materials, and (d) the device configuration.

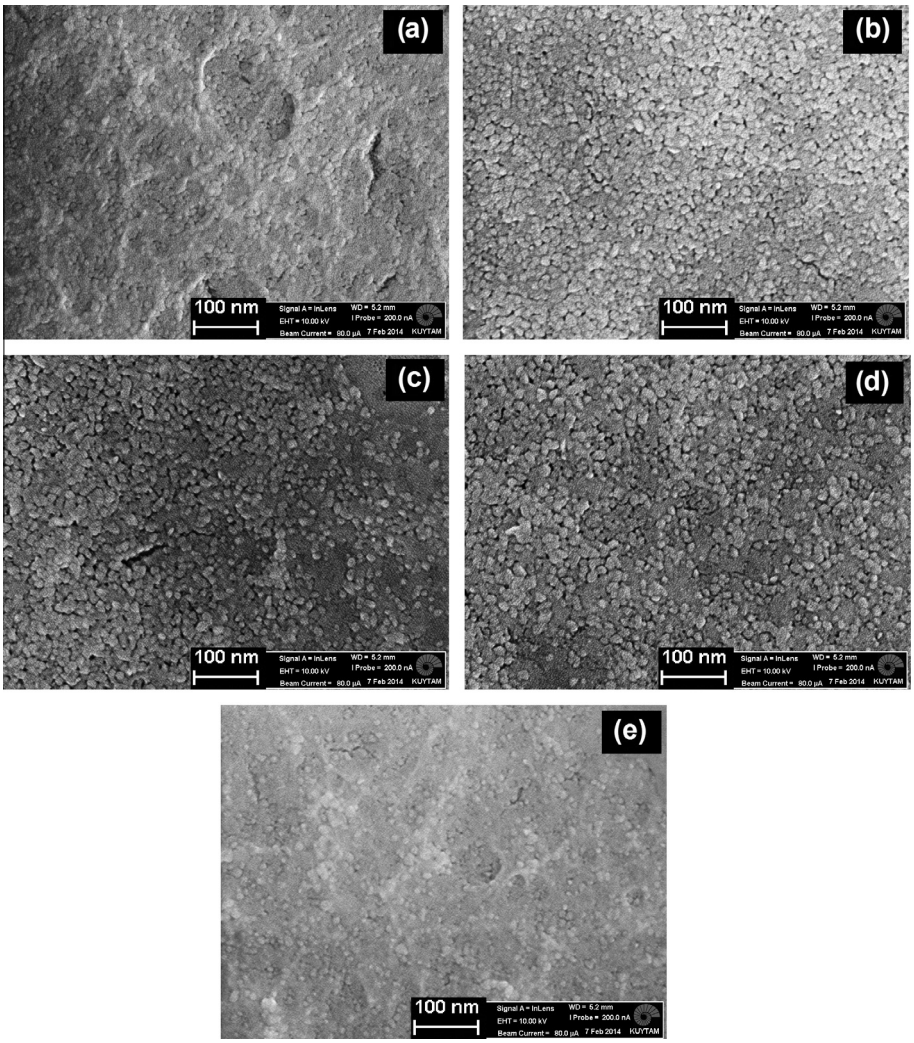

Fig. 2. SEM images of undoped and Fe doped TiO_2 thin films; (a) undoped, (b) 0.5%, (c)1%, (d) 2%, and (e) 3% Fe doped TiO_2 thin films.

granular structure are becoming more aperient with Fe doping in the TiO_2 at 0.5%, 1% and 2% doping ratios. However, granules getting smaller at 3% doping ratio and the morphology shift to a more smooth film structure.

Optical absorption spectra are a nice tool to calculate the band gap of the semiconductors. Basically, absorption determines the electron excitation from valance band to conduction band, which can be used for calculation of

the band gap. The relationship between absorption coefficient (α) and incident photon energy ($h\nu$) in fact is given by following equation for allowed indirect transitions.

$$(\alpha h\nu) = A(h\nu - E_g)^2$$

where A is a constant, E_g is the band gap of the material, ν is the frequency of the photons and h is the Planck's constant. $(\alpha h\nu)^2$ versus $h\nu$ plot of Fe doped and pure TiO_2 thin films given in Fig. 3. The optical band gap of doped and pure TiO_2 thin films has been calculated from the above equation, which gives the band gap (E_g), when linear portion of $(\alpha h\nu)^2$ against $h\nu$ plot is extrapolated to the point $\alpha = 0$. The changes of the band gap with respect to the Fe^{2+} concentrations are also given in Fig. 3 as inset. It is clearly seen that from Fig. 3 absorption is shifting firstly to higher energy levels so band gap of the small amount Fe^{2+} doped samples is increasing and then it is decreasing for higher Fe^{2+} concentrations. There are numerous studies related to the Fe^{2+} doped TiO_2 thin films in the literature (Wang et al., 2009; Lin et al., 2012; Wang et al., 2013). Red-shift in the absorption spectra in high Fe concentration is not originally related to Fe concentration; however, it can be explained by the structural changes from anatase to rutile due to the iron concentration in the TiO_2 lattice (Bally et al., 1998). Blue-shift is observed with low Fe concentration, which can be explained by the Burstein–Moss shift (Burstein, 1954).

The crystal structure of pure and Fe doped TiO_2 thin films were analyzed with X-ray diffraction (XRD). XRD pattern of pure and Fe doped TiO_2 thin films on the Y axis offset were given in Fig. 4. It is clearly seen that form Fig. 4, all the diffraction peaks of doped and undoped samples belong to anatase phase TiO_2 structure and no other phase can be detected. Moreover, it can be observed from Fig. 4 that intensity of diffraction peaks decreases with increases Fe concentration in the TiO_2 lattice. It can be attributed that Fe impurities disrupt the crystal structure of the anatase TiO_2.

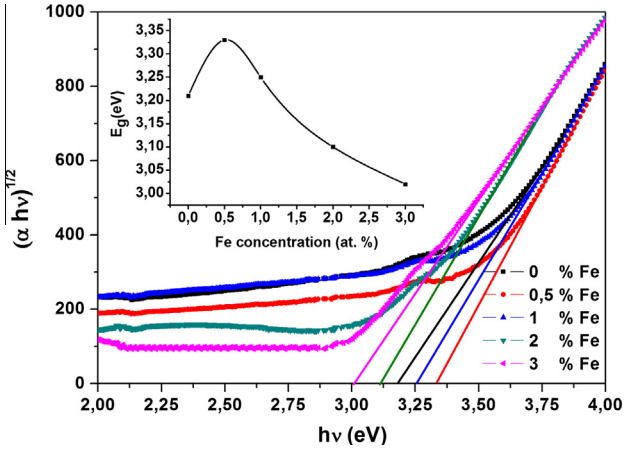

Fig. 3. Graphs of $(\alpha h\nu)^{1/2}$ versus $h\nu$ of TiO_2 and Fe:TiO_2. The changes of band gap according to Fe concentration as inset.

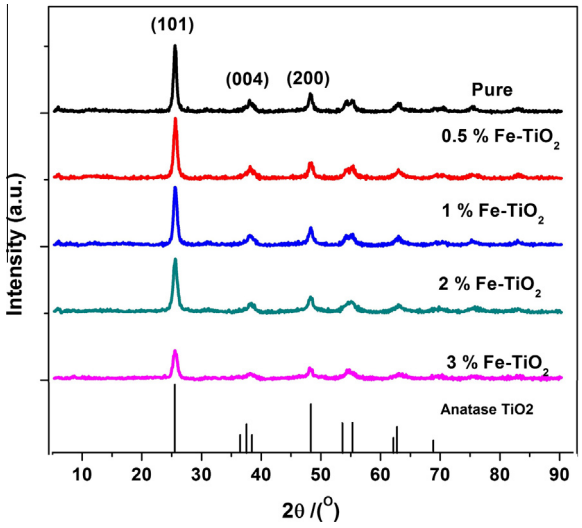

Fig. 4. X-ray diffraction spectra of the Fe-doped TiO_2 thin films with the standard differential peaks of anatase TiO_2 (JCPDS No. 21-1272).

The surface properties of the Fe doped and undoped TiO_2 films were studied by X-ray Photoelectron Spectroscopy (XPS). Fig. 5 shows the XPS survey spectra of 1% Fe doped TiO_2 thin films. The XPS peaks show that the Fe doped TiO_2 films contains Ti, O, C, and Fe elements. The XPS peaks at 458.28, 529.72 and 285.5 eV are attributed to Ti 2p, O 1s, C 1s and 708.5 eV correspond to binding energy of Fe 2p. In order to demonstrate iron content in the TiO_2, the Fe 2p core level XPS spectra are given in Fig. 5 as inset. Fig. 5 shows that the peaks intensity is increasing with Fe concentration.

TiO_2 is in fact an intrinsic oxide semiconductor material and has n type conductivity. However, when it is doped with iron atoms, its conductivity converts to a p type behavior, because Fe impurities act as acceptor impurities in the TiO_2 crystal (Bally et al., 1998). Bally et al. (1998) reported that Fe atoms don't behave as simple substitutional defects, which replace Ti atoms in the crystal

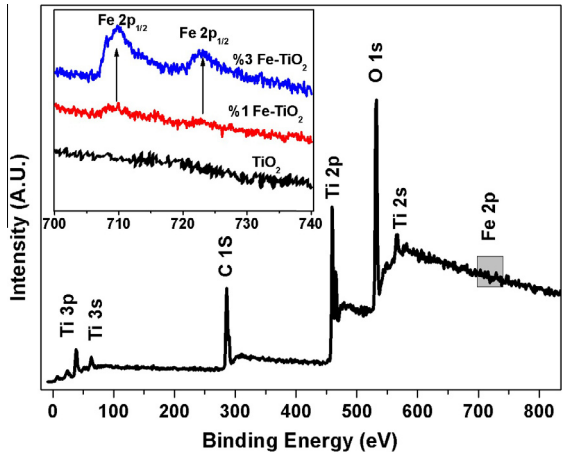

Fig. 5. Core level XPS spectra for the 1% Fe doped TiO_2 thin films. The Fe $2p_{1/2}$ and $2p_{3/2}$ spectra for the 0%, 1% and 3% Fe doped TiO_2 samples is given as inset.

Table 1
Performance parameters of the solar cells produced with pure and Fe doped solar TiO_2 thin films.

Fe doping ratio (%)	FF (%)	V_{oc} (V)	I_{sc} (mA/cm^2)	η (%)
0	0.3665	0.53	8.75	1.7
0.5	0.3673	0.55	10.89	2.19
1	0.3689	0.55	13.8	2.78
2	0.4231	0.51	9.28	1.98
3	0.4125	0.41	7.68	1.29

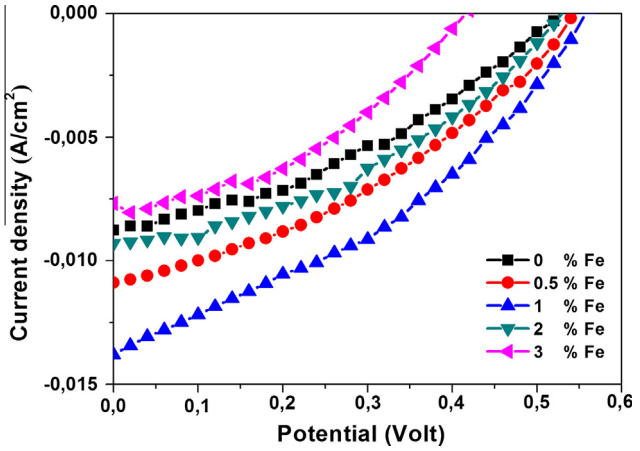

Fig. 6. J–V characteristics of inverted type solar cells fabricated with TiO_2 and Fe doped TiO_2 electron transport layers.

structure. They claimed that in their work the samples with the lowest concentration Fe atoms shows n type conductivity higher than undoped samples because of the new oxygen vacancies produced by the iron atoms in the oxide lattice (Sayle et al., 1995). The increased band gap at 0.5% and 1% Fe concentration may be attributed to the new oxygen vacancies induced by Fe atoms in the lattice.

The most important part of the inverted type solar cells is the electron transport layer and TiO_2 is a famous material that are used as an electron selective layer in the inverted type solar cell structure. In order to improve the electron transport and hole blocking properties of TiO_2 layer, it is typically doped with some metal ions. There are various investigations about the effect of the dopant ions in the TiO_2 layer. For instance, Ranjitha and co-workers doped TiO_2 with Cd ions, which led to improvement in solar cell efficiency. This was explained by the improved electron transport properties of the TiO_2 by Cd doping (Ranjitha et al., 2014). Sn-doped TiO_2 was used by Thambidurai and co-workers as an electron selective layer and they could have improved the solar cell parameters indeed (Thambidurai et al., 2014). In addition, Zn was also used as a dopant ion to improve the solar cell efficiency (Thambidurai et al., 2014). However, there is no any study about the using of Fe doped TiO_2 thin films as electron transport layer for inverted type solar cells.

In this study, we have mainly investigated, what is the effect of Fe doping of TiO_2 in inverted type solar cell efficiency. Electrical and optical properties of the Fe doped TiO_2 thin films were investigated by many research groups. It is well known that Fe impurities act as acceptor impurities in the TiO_2 lattice. Thus, at the first glance, it can be considered that Fe doped TiO_2 cannot be used as an electron selective layer due to the fact that acceptor impurities induced iron atoms act as trap levels for the electrons from active layer. However, at low Fe concentrations, n type properties of TiO_2 are improved (Sayle et al., 1995). Fig. 4 illustrates the current–voltage characteristic of the inverted type solar cells fabricated with undoped and Fe doped TiO_2 thin films under the illumination of AM 1.5 and solar cell parameters. These results are shown in Table 1. From the J–V characteristics a dramatic increase

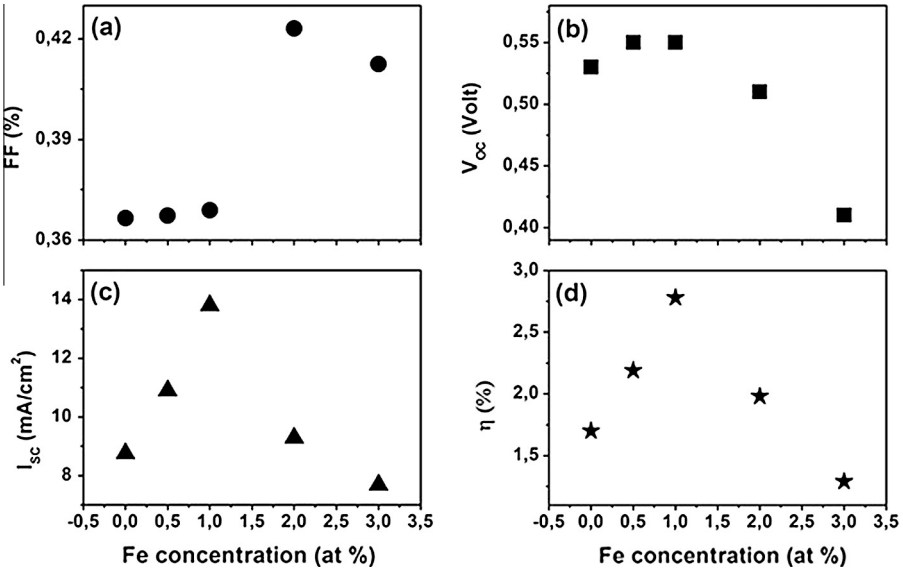

Fig. 7. Dependency of Solar cell parameters on the Fe concentration in TiO_2 structure (a) fill factor; (b) open circuit voltage; (c) short circuit current; and (d) power conversion efficiency.

was observed in the J_{SC} from 8.75 mA/cm^2 to 13.8 mA/cm^2 with the 1% Fe doped TiO_2 solar cell sample. When the concentration of Fe impurities in the TiO_2 lattice was increased to higher than 1%, current density was diminished suddenly, as expected. Fill factor showed slight increase as well up to 1% Fe doping ratio. After this value, there is a negligible change in open circuit voltage values until 1% doping, but suddenly a decrease observed at higher concentrations.

To obtain a better overview of the effect of Fe impurities in the TiO_2 layer, photovoltaic parameters such as FF, V_{oc}, I_{sc} and η% was systematically studied and the results are shown in Fig. 5. It is clearly seen that, I_{sc} and V_{oc} are increased by increasing of Fe concentration up to 1% and then sudden decrease was observed for higher concentration for both. Similarly, the solar cell efficiency increased from 1.7% to 2.79% with 1% Fe doping ratio and it suddenly decreased to 1.29% with 3% doping ratio (see Figs. 6 and 7).

4. Conclusion

Inverted P3HT:PCBM based organic solar cells were fabricated by using Fe^{2+} doped TiO_2 films as electron selective layer in this work. The goal of our work was principally to present a quantitative and valuable optimization, which encourages the possible implantations of similar kind of doping in similar applications. Major findings are summarized as follows; Pure and Fe^{2+} doped TiO_2 layers were successfully prepared on ITO substrate. Granular structure was observed with Fe doping in the TiO_2 layer at 0.5%, 1% and 2% doping ratios. However, the morphology shifted to smooth structure at 3% doping ratio. Band gap was increased at 0.5% and 1% Fe^{2+} concentrations, which was attributed to the new oxygen vacancies induced by Fe atoms in the lattice. A dramatic increase was observed in the J_{SC} from 8.75 mA/cm^2 to 13.8 mA/cm^2 with the 1% Fe doped TiO_2 solar cell sample. I_{sc} and V_{oc} showed maximum values at 1% Fe^{2+} concentration and solar cell efficiency of 2.78% was obtained.

Acknowledgement

This research is supported by TUBITAK Grant No.: 113M935.

References

Alparslan, Z., Kösemen, A., Ornek, O., Yerli, Y., San, S.E., 2011. TiO_2-based organic hybrid solar cells with Mn^{+2} doping. Int. J. Photoenergy 10, 8 page Article ID 734618.

Andersen, T.R., Dam, H.F., Hosel, M., Helgesen, M., Carle, J.E., Larsen-Olsen, T.T., Gevorgyan, S.A., Andreasen, J.W., Adams, J., Li, N., Machui, F., Spyropoulos, G.D., Ameri, T., Lemaitre, N., Legros, M., Scheel, A., Gaiser, D., Kreul, K., Berny, S., Lozman, O.R., Nordman, S., Valimaki, M., Vilkman, M., Søndergaard, R.R., Jørgensen, M., Brabec, C.J., Krebs, F.C., 2014. Scalable, ambient atmosphere roll-to-roll manufacture of encapsulated large area, flexible organic tandem solar cell modules. Energy Environ. Sci. 7, 2925–2933.

Bally, A.R., Korobeinikovax, E.N., Schmidy, P.E., Lévyy, F., Bussyk, F., 1998. Structural and electrical properties of Fe-doped TiO_2 thin films. J. Phys. D: Appl. Phys. 31, 1149–1154.

Burstein, E., 1954. Anomalous optical absorption limit in InSb. Phys. Rev. 93, 632.

Cheng, Y.J., Cao, F.Y., Lin, W.C., Chen, C.H., Hsieh, C.H., 2011. Self-assembled and cross-linked fullerene interlayer on titanium oxide for highly efficient inverted polymer solar cells. |Chem. Mater. 23, 1512–1518.

de Jong, M.P., van Ijzendoorn, L.J., de Voigt, M.J.A., 2000. Stability of the interface between indium-tin-oxide and poly(3,4-ethylene-dioxythiophene)/poly(styrenesulfonate) in polymer light-emitting diodes. Appl. Phys. Lett. 77, 2255.

Girtan, M., Rusu, M., 2010. Role of ITO and PEDOT:PSS in stability/degradation of polymer:fullerene bulk heterojunctions solar cells. Sol. Energy Mater. Sol. Cells 94, 446–450.

Hames, Y., Alpaslan, Z., Kösemen, A., San, S.E., Yerli, Y., 2010. Electrochemically grown ZnO nanorods for hybrid solar cell applications. Sol. Energy 84, 426–431.

Kawano, K., Pacios, R., Poplavskyy, D., Nelson, J., Bradley, D.D.C., Durrant, J.R., 2006. Degradation of organic solar cells due to air exposure. Sol. Energy Mater. Sol. Cells 90, 3520–3530.

Kim, R., Cho, S., Park, W.G., Cho, D.Y., Oh, S.-J., Martin, R.S., Berthet, P., Park, J.G., Yu, J., 2014. Charge and magnetic states of rutile TiO_2 doped with Cr ions. J. Phys.: Condens. Matter 26, 146003.

Kuwabara, T., Nakayama, T., Uozumi, K., Yamaguchi, T., Takahashi, K., 2008. Highly durable inverted-type organic solar cell using amorphous titanium oxide as electron collection electrode inserted between ITO and organic layer. Sol. Energy Mater. Sol. Cells 92, 1476–1482.

Li, G., Chu, C.W., Shrotriya, V., Huang, J., Yang, Y., 2006. Efficient inverted polymer solar cells. Appl. Phys. Lett. 88, 253503.

Liang, Y., Xu, Z., Xia, J., Tsai, S.T., Wu, Y., Li, G., Ray, C., Yu, L., 2010. For the bright future—bulk heterojunction polymer solar cells with power conversion efficiency of 7.4%. Adv. Mater. 22, 135–138.

Liao, H.H., Chen, L.M., Xu, Z., Li, G., Yang, Y., 2008. Highly efficient inverted polymer solar cell by low temperature annealing of Cs_2CO_3 interlayer. Appl. Phys. Lett. 92, 173303.

Lin, Y.H., Yang, P.C., Huang, J.S., Huang, G.D., Wang, I.J., Wu, W.H., Lin, M.Y., Su, W.F., Lin, C.F., 2011. High-efficiency inverted polymer solar cells with solution-processed metal oxides. Sol. Energy Mater. Sol. Cells 95, 2511–2515.

Lin, C.Y.W., Channei, D., Koshy, P., Nakaruk, A., Sorrell, C.C., 2012. Effect of Fe doping on TiO_2 films prepared by spin coating. Ceram. Int. 38, 3943–3946.

Liu, C., Chen, H., Zhao, D., Shen, L., He, Y., Guo, W., Chen, W., 2014. The action mechanism of TiO_2:$NaYF_4$:Yb^{3+}, Tm^{3+} cathode buffer layer in highly efficient inverted organic solar cells. Appl. Phys. Lett. 105, 053301.

Norrman, K., Larsen, N.B., Krebs, F.C., 2006. Lifetimes of organic photovoltaics: combining chemical and physical characterisation techniques to study degradation mechanisms. Sol. Energy Mater. Sol. Cells 90, 2793–2814.

Norrman, K., Madsen, M.V., Gevorgyan, S.A., Krebs, F.C., 2010. Degradation patterns in water and oxygen of an inverted polymer solar cell. J. Am. Chem. Soc. 132, 16883–16892.

Peumans, P., Yakimov, A., Forrest, S.R., 2003. Small molecular weight organic thin-film photodetectors and solar cells. J. Appl. Phys. 93, 3693.

Ranjitha, A., Muthukumarasamy, N., Thambidurai, M., Velauthapillai, Dhayalan, Kumar, A.M., Gasem, Z.M., 2014. Inverted organic solar cells based on Cd-doped TiO_2 as an electron extraction layer. Superlattices Microstruct. 74, 114–122.

Sayle, D.C., Catlow, C.R.A., Perrin, M.-A., Nortier, P., 1995. J. Phys. Chem. Solids 56, 799.

Su, Yu-Wei, Lan, Shang-Che, Wei, Kung-Hwa, 2012. Organic photovoltaics. Mater. Today 15, 554.

Thambidurai, M., Kim, J.Y., Song, H.J., Ko, Y., Muthukumarasamy, N., Velauthapillai, D., Bergmann, V.W., Weberd, S.A.L., Lee, C., 2014. Enhanced power conversion efficiency of inverted organic solar cells by using solution processed Sn-doped TiO_2 as an electron transport layer. J. Mater. Chem. A 2, 11426–11431.

Thambidurai, M., Kim, J.Y., Ko, Y., Song, H.-J., Shin, H., Song, J., Lee, Y., Muthukumarasamy, N., Velauthapillaic, D., Lee, C., 2014. High-efficiency inverted organic solar cells with polyethylene oxide-modified Zn-doped TiO_2 as an interfacial electron transport layer. Nanoscale 6, 8585.

Wang, M.C., Lin, H.J., Yang, T.S., 2009. Characteristics and optical properties of iron ion (Fe^{3+})-doped titanium oxide thin films prepared by a sol–gel spin coating. J. Alloys Comp. 473, 394–400.

Wang, C.-T., Siao, H.-L., Chiu, Y.-C., 2013. Iron-doped titania thin films with enhanced photovoltaic efficiency: effects of iron concentration and rectifying layer. Surf. Coat. Technol. 232, 658–665.

Winkler, T., Schmidt, H., Flügge, H., Nikolayzik, F., Baumann, I., Schmale, S., Weimann, T., Hinze, P., Johannes, H.-H., Rabe, T., Hamwi, Riedl, T., Kowalsky, W., 2011. Efficient large area semitransparent organic solar cells based on highly transparent and conductive ZTO/Ag/ZTO multilayer top electrodes. Org. Electron. 12, 1612–1618.

Wong, K.H., Mason, C.W., Devaraj, S., Ouyang, J., Balaya, P., 2014. Low temperature aqueous electrodeposited TiOx thin films as electron extraction layer for efficient inverted organic solar cells. Appl. Mater. Interfaces 6, 2679–2685.

Xu, M.F., Zhu, X.Z., Shi, X.B., Liang, J., Jin, Y., Wang, Z.K., Liao, L.S., 2013. Plasmon resonance enhanced optical absorption in inverted polymer/fullerene solar cells with metal nanoparticle-doped solution-processable TiO2 layer. Appl. Mater. Interfaces 5, 2935–2942.

Yu, G., Gao, J., Hummelen, J.C., Wudl, F., Heeger, A.J., 1995. Polymer photovoltaic cells: enhanced efficiencies via a network of internal donor–acceptor heterojunctions. Science 270, 1789.

Yu, B.Y., Tsai, A., Tsai, S.P., Wong, K.T., Yang, Y., Chu, C.W., Shyue, J.J., 2008. Efficient inverted solar cells using TiO_2 nanotube arrays. Nanotechnology 19, 255202.

Yuan, B., Wang, Y., Bian, H., Shen, T., Wu, Y., Chen, Z., 2013. Nitrogen doped TiO_2 nanotube arrays with high photoelectrochemical activity for photocatalytic applications. Appl. Surf. Sci. 280, 523–529.